Microscopic theory of the ^{4}He system with multichannel resonating-group method

H. Kanada and T. Kaneko
Department of Physics, Niigata University, Niigata 950-21, Japan

Y. C. Tang
School of Physics, University of Minnesota, Minneapolis, Minnesota 55455

(Received 10 January 1986)

The ground and even-parity excited states and the scattering problem of the ^{4}He system are examined within the framework of the (2N + 2N) and (1N + 3N) cluster-coupling model with the specific distortion effect of the deuteron cluster taken into consideration. Calculations are performed by a multichannel resonating-group method using an effective nucleon-nucleon (NN) potential similar to that adopted in p + α, d + α, ^{3}H + α (or ^{3}He + α), and α+α systems. The results show that, because of the high compressibility of the deuteron cluster and the similarity in threshold energies for the 2N + 2N and 1N + 3N configurations, both the distortion effect and the channel-coupling effect are important in this system. When the 1N + 3N configuration is included in the calculation, the deuteron-distortion effect turns out to be significantly weakened, owing to the fact that the 1N + 3N configuration is energetically the most favored one. In addition, it is shown that such a specific distortion effect is quite small in the channel spin $S=2$ state of d+d scattering. With the full calculation including the distortion effect, it is found possible to reproduce well the energies of the ground state and the first-excited 0^+ state; the differential cross sections for d+d, p+t, and n+h elastic scattering; the polarizations for p+t and n+h scattering; and the cross sections for ^{1}H(t,n)^{3}He and ^{3}H(p,d)^{2}H reactions.

I. INTRODUCTION

Recently,[1-3] we have shown that the d+α system can be reasonably described by taking into account the effects of specific distortion of the deuteron cluster which has high compressibility. By a careful consideration of these effects, both the ^{6}Li bound-state and the low-energy d+α scattering data can be well explained. In addition, the results show that the effective NN potential required is very similar to that employed in studies of p+α, ^{3}He+α (^{3}H+α), and α+α systems.[1-5] This is an interesting finding from the viewpoint of a unified description of the behavior of light nuclear systems. Additionally, it has been shown in Ref. 3 that the multichannel R-matrix theory with a variational method can be successfully applied to study the specific distortion effect and/or the channel-coupling effect in few-nucleon problems.

The ^{4}He system is the lightest nucleus which is interesting in many respects. It has many excited odd- and even-parity states, and many cluster configurations such as p+t, n+h, and d+d configurations have threshold energies which are very close to one another.

In this investigation, the ^{4}He system will be considered by including both the specific distortion effect of the deuteron cluster and the coupling effect among the various channels. To take these effects into account, we adopt the same type of trial wave function as that described in Refs. 1–3, i.e., the multichannel resonating-group method (MCRGM). For all clusters (d, t, and h), flexible normalized two- or three-Gaussian functions will be used.

Theoretical investigations of the ^{4}He system have already been carried out by other authors. Heiss *et al.* and Hofmann *et al.*[6] performed p+t, n+h, and d+d coupled-channel calculations and reproduced rather successfully the experimental data both for elastic and reaction processes. However, in their calculations, the specific distortion effect of the deuteron was not taken into account. Furutani[7] studied the ^{4}He system within the framework of the (1N + 3N)-cluster model using the generator-coordinate method and succeeded in reproducing the negative-parity levels, but not the positive-parity level structure because of the lack of consideration of the d+d channel. Thompson[8] studied the d+d scattering system utilizing a single-channel RGM and showed that even such a simple treatment can reproduce fairly the differential cross section in the low-energy region.

To supplement the above-mentioned investigations, we feel that it will be useful to carry out a more complete study by including not only the specific-distortion effect of the deuteron cluster but also all relevant two-cluster configurations. In particular, we will be interested in studying the effect of the d+d configuration on the positive-parity states and the scattering properties. As in the d+α case, the MCRGM will again be adopted, with an effective NN potential (Minnesota or MN potential) similar to that required in other light nuclear systems.

In the next section, we present a brief description of the MCRGM (or MC R-matrix theory) and the choice of cluster internal wave functions. Section III is devoted to a detailed discussion of the results for the bound state, excited state, and scattering states, obtained in various cases of channel coupling. Calculated differential cross sections for d+d, p+t, and n+h elastic scattering and polarizations for p+t and n+h scattering are also discussed in

Sec. III. Finally, in Sec. IV, concluding remarks are made.

II. FORMULATION

For the formulation of the present problem, we adopt the multichannel R-matrix theory as described fully in Ref. 3. Hence, only a brief discussion will be given here.

In the present calculation of the ^{4}He system, all two-cluster fragmentations are taken into account, i.e., 2N + 2N and 1N + 3N configurations. The total wave function of the ^{4}He system for a given total angular momentum J and channel spin S is written as the following superposition:

$$\Psi_{JS}=\mathscr{A}\left[\sum_c \psi_c^{Jl,S}(R_c)\,|\,c\rangle\right], \tag{2.1}$$

where $\psi^{Jl,S}(R_c)$ is the radial part of the relative wave function between two nuclei in channel c which, in the present study, denotes the channel d+d, d*+d, d*+d*, d**+d, d**+d*, d**+d**, p+t, or n+h, with R_c representing the relative distance between them, and l is the intercluster orbital angular momentum. The ket $|\,c\rangle$ denotes the channel wave function in channel c and is described by the internal wave functions $\Phi^A_{\alpha_A}$ and $\Phi^B_{\alpha_B}$ for clusters A and B with quantum numbers α_A and α_B; it is given by

$$|\,c\rangle=(\{\Phi^A_{\alpha_A}\Phi^B_{\alpha_B}\}_S Y_l)_J\ . \tag{2.2}$$

The total wave function is completely antisymmetrized. By using the standard resonating-group procedure, one can obtain coupled integro-differential equations for the eight relative wave functions ψ_c as follows:

$$\sum_{c'}\int_0^\infty R_c'^2 dR_{c'}'[H_{cc'}(R_c,R_{c'}')-EN_{cc'}(R_c,R_{c'}')]\psi_{c'}(R_{c'}')=0\ , \tag{2.3}$$

where E is the total energy of the system, $H_{cc'}(R_c,R_{c'}')$ is the energy kernel, and $N_{cc'}(R_c,R_{c'}')$ is the norm kernel.

In the R-matrix theory, the inside solution of Eq. (2.3) ($R_c\leqq a_c$, with a_c the channel radius) can be obtained by introducing the Bloch operator and by using a variational method[9] as discussed in Ref. 3. Adopting suitable boundary conditions on the relative wave functions and using the outside solution, one can then obtain the R matrix and, consequently, the S matrix (see Ref. 1).

For the internal wave functions of d, t, and h clusters appearing in Eq. (2.2), same types of flexible normalized N_A-Gaussian functions are adopted; i.e., for an A cluster we use

$$\Phi^A=\sum_{j=1}^{N_A} C_j^A\Phi_j^A\ , \tag{2.4}$$

where Φ_j^A is taken as

$$\Phi_j^A=\exp\left[-\tfrac{1}{2}\lambda_j^A\sum_i^A(\mathbf{r}_i-\mathbf{R}_A)^2\right]\quad(j=1\text{ to }N_A)\ . \tag{2.5}$$

The variational parameters (C_j and λ_j) for each cluster are obtained by minimizing the expectation value of the cluster Hamiltonian. It should be noted that, with this procedure, the resultant cluster wave functions do satisfy the variational stability conditions. In the deuteron case, N_2 is set as 3, and for the t and h clusters, N_3 is chosen equal to 2. The excited deuteron configurations Φ(d*) and Φ(d**) are obtained as eigenstates of the cluster Hamiltonian in the space spanned by the three Gaussian functions with λ_i values of the ground state. The parameters obtained for all the clusters appearing in the present study are listed in Table I, together with the expectation values of the cluster Hamiltonians and the rms radii. The NN potential V_{ij} employed has the same form as that adopted in Refs. 1 and 5; it contains two parameters u and c_s, which are chosen here to be $u=1$ and $c_s=1$, as indicated from the study of p+α scattering by Furber[10] [see Eqs. (12)–(17) in Ref. 5].

TABLE I. Results of variational calculation for Φ_d, Φ_t, and Φ_h.

Cluster	Width parameter λ_i (fm^{-2})	Expectation value of Hamiltonian (MeV)	$(\langle r^2\rangle)^{1/2}$ (fm)
d	(0.049, 0.224, 1.004)	−2.084	1.984
		3.158	4.30
		27.790	2.29
t	(0.1899, 0.639)	−5.831	1.683
		12.546	2.256
h	(0.1845, 0.63)	−5.091	1.708
		12.655	2.278

III. CALCULATED RESULTS

A. Cases of calculations

In this calculation, because of the importance of the specific distortion effect of the deuteron, we introduce six channels for the 2N + 2N configuration as d+d, d*+d, d*+d*, d**+d, d**+d*, and d**+d** channels. Here, the five pseudoinelastic channels (d*+d, d*+d*, d**+d, d**+d*, and d**+d**) which include excited deuterons will be taken to satisfy asymptotic boundary conditions of real channels. Further, we introduce two channels as p+t and n+h ones for the 1N + 3N configuration.

To reduce computational effort, we have made the simplification of omitting channel-spin mixing effects arising from the presence of a spin-orbit component in the NN potential. This is a reasonable approximation to make, since the calculation of Hofmann *et al.*[6] showed that the channel-spin mixing parameter is very small in the low-energy region. Similar conclusion has been reached by Tombrello[11] from a phase-shift analysis of the p+h scattering data. With this simplification, there exists then only coupling between the 1N + 3N and 2N + 2N configurations in channel spin $S=0$ and 1 states, but not in the channel spin $S=2$ state.

To investigate the channel-coupling effect and/or the

TABLE II. Calculated energies for the ground and the first-excited states of ^{4}He with the Minnesota potential in $3G_d$-$2G_{3N}$ Model.

Configuration	Case	Ground 0^+ (MeV)	Excited 0^+ (MeV)
(dd)	SC	−19.21	−3.22
(dd) + (d*d)	DC1	−21.52	−3.53
(dd) + (d*d*)	DC2	−19.55	−3.31
(dd) + (d*d) + (d*d*)	TC1	−21.90	−3.68
(dd) + (d*d) + (d*d*) + (d**d) + (d**d*) + (d**d**)	Sext.C1	−23.02	−3.91
(pt) + (nh)	DC3	−25.17	−5.10
(pt) + (nh) + (dd)	TC2	−26.03	−5.98
(pt) + (nh) + (dd) + (d*d)	Quad.C1	−26.20	−6.00
(pt) + (nh) + (dd) + (d*d*)	Quad.C2	−26.03	−6.07
(pt) + (nh) + (dd) + (d*d) + (d*d*)	Quint.C	−26.28	−6.10
(pt) + (nh) + (dd) + (d*d) + (d*d*) + (d**d)	Sext.C2	−26.34	−6.17
(pt) + (nh) + (dd) + (d*d) + (d*d*) + (d**d) + (d**d*)	Sep.C	−26.39	−6.38
(pt) + (nh) + (dd) + (d*d) + (d*d*) + (d**d) + (d**d*) + (d**d**)	OC (full)	−26.50	−6.43
Experiment		−28.3	−8.3

specific distortion effect of the deuteron cluster, we shall perform calculations in a variety of cases. These cases are listed in the second column of Table II.

B. Ground state and first-excited 0^+ state

We examine the ground state (0^+) and first-excited positive-parity state (0^+) in the ^{4}He system.[12] By Furutani[7] and Sakai *et al.*,[13] it has been shown that the 1N + 3N configuration plays an important role in reproducing the negative-parity states in ^{4}He. Therefore, we shall concentrate here on examining the interplay between the 1N + 3N and the 2N + 2N configurations regarding the manner in which the level structure of the positive-parity states can be explained.

The results calculated for the ground state of ^{4}He are listed in Table II. In this table, one can find several interesting facts. In the cases where only the 2N + 2N configurations are taken into account, the specific distortion effect of the deuteron plays an important role; on the other hand, by introducing the 1N + 3N configuration, this effect is greatly weakened. This indicates that, for the ground state of ^{4}He, the 1N + 3N configuration is more important than the 2N + 2N configuration, and the properties of the dd system are strongly affected by the presence of pt and nh configurations.

The results calculated for the first-excited state of ^{4}He are also listed in Table II and compared with experimental data.[14–16] One can see from this table that the full calculation (eight-channel calculation) reproduces fairly well the energy of the first-excited level of ^{4}He, and that the effect of including pseudoinelastic configurations is not too large, but still cannot be neglected.

From Table II, one also finds the following interesting features:

(i) With a trial function of the form given by Eq. (2.4) which does not take cluster correlations explicitly into account, one obtains with $N_4 = 15$ a ground-state energy expectation value of −25.55 MeV, which is larger than the value of −26.50 MeV obtained in the full calculation. This indicates that, even for a nucleus as light as ^{4}He, a proper consideration of clustering effects is important.

(ii) The p+t plus n+h cluster configuration, to be referred to collectively as the 1N + 3N cluster configuration, is the dominant component in both the ground and the first-excited 0^+ states of ^{4}He.

(iii) The d+d cluster configuration plays a significant role; it lowers the energies by 0.86 and 0.88 MeV in the ground and first-excited 0^+ states, respectively. On the other hand, the pseudoinelastic configurations involving excited deuteron states seem to have only moderate influence. The addition of these latter configurations improves the energy by 0.47 and 0.45 MeV in the ground state and the first-excited state, respectively.

(iv) The importance of pseudoinelastic configurations depends on whether or not the 1N + 3N configuration is included in the calculation. This shows that, when the energetically most favored 1N + 3N configuration is not explicitly accounted for, its effect may be partially compensated for by the addition of pseudodeuteron configura-

tions. However, it should be pointed out that this particular way of improving the behavior of the compound system in the strong-interaction region is quite inefficient. Rather, one should always adopt the viewpoint that, for a proper understanding of the characteristics of a nuclear system, the energetically most favored cluster configuration must be taken into consideration.

For an understanding of the role played by channel coupling in the ground-state wave function, the R_c dependences of the relative wave functions f_G, equal to $R_c\psi_c^{00,0}$ [see Eq. (2.1)], for both 2N + 2N and 1N + 3N configurations, are calculated. The results are shown as a function of $R_c = nh$ with $h = 0.26$ fm in Fig. 1. In Figs. 1(a), 1(b), and 1(c) the wave functions for the 2N + 2N configurations are shown in cases SC, DC1, and TC1, respectively. The wave functions of the p+t and n+h configurations obtained in case DC3 are shown in Fig. 1(d). The wave functions for the three-configuration calculation in case TC2 are shown in Fig. 1(e), while those for all configurations obtained in the octuple-configuration calculation (case OC) are shown in Fig. 1(f). In the latter figure, the wave functions for the $d^{**}+d$ and $d^{**}+d^*$ configurations, which are of the same order as the $d^{**}+d^{**}$ wave function, are not shown in order to avoid confusion.

By comparing the results shown in all these figures, one can see the following characteristic features:

(i) In the calculation with 2N + 2N configurations, the d+d channel yields the main component of the ground-state wave function. Both the d^*+d and d^*+d^* components do not have large magnitudes in the inner region, but even the component of the d^*+d^* channel is not negligible.

(ii) As seen from Fig. 1(d), the wave function for the p+t configuration has a larger contribution in the inner region, while that for the n+h configuration has a larger contribution in the outer region. Also, a node appears in the nh wave function [see also Figs. 1(e) and 1(f)]. This is an indication that, in the ground state of ^{4}He, there is an appreciable contribution from higher shell-model configurations, such as 2p-2h configurations.

(iii) In Figs. 1(e) and 1(f) it is seen that, in both inner and outer regions, the summed magnitudes of the two wave functions for the 1N + 3N configuration are larger than the magnitude of f_G(dd), indicating, by the presence of the 1N + 3N configuration, that the component for 2N + 2N configuration is pushed to the outer region and its amplitude becomes smaller in the whole region than that obtained in the case where the 2N + 2N configuration alone is considered. This shows that the 1N + 3N configuration contributes most to the ground state of the ^{4}He system. However, it is also shown from this investigation that even in this case the contribution of pseudoinelastic channels is still somewhat important and should be properly taken into consideration.

Although one cannot exactly interpret these wave functions as relative probability amplitudes because of an-

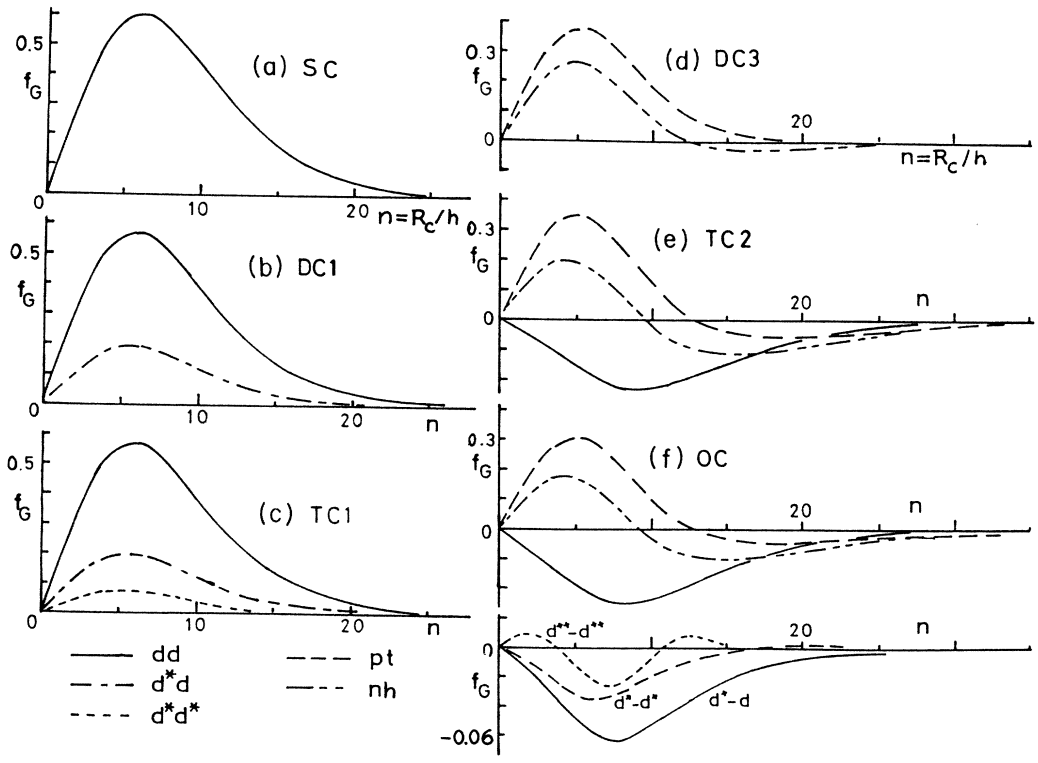

FIG. 1. Relative-motion wave functions in the ground state of the ^{4}He system with 2N + 2N configuration [parts (a), (b), and (c)]. In part (d) the behavior of the R_c-dependent relative-motion wave function in 1N + 3N configuration is shown. In parts (e) and (f) relative-motion wave functions are obtained with (1N + 3N) + (2N + 2N) configurations.

TABLE III. Calculated rms charge radius $\tilde{R}_{\alpha,\mathrm{ch}}$ of ^{4}He.

Configuration	Case	$\tilde{R}_{\alpha,\mathrm{ch}}$ (fm)
(dd)	SC	2.200
(pt) + (nh)	DC3	1.607
(pt) + (nh) + (dd)	TC2	1.694
(pt) + (nh) + (dd) + (d*d) + (d*d*)	Quint.C	1.658
(pt) + (nh) + (dd) + (d*d) + (d*d*) + (d**d) + (d**d*) + (d**d**)	OC (full)	1.593
Experimental value:	$\tilde{R}^{\mathrm{expt}}_{\alpha,\mathrm{ch}}=1.63\pm0.04$ fm	

tisymmetrization, the above observations do show that the distortion and/or channel-coupling effects are very important in the ^{4}He system.

Using the optimum ground-state wave function, we can calculate the rms charge radius $\tilde{R}_{\alpha,\mathrm{ch}}$ of ^{4}He. Results obtained with various configurations are shown in Table III, where the experimental value of $\tilde{R}_{\alpha,\mathrm{ch}}$ (Ref. 17) is also listed. One finds from this table that the effect of the 2N + 2N configuration is fairly large and the contribution of pseudoinelastic configurations including excited deuteron states is rather important. The agreement between the calculated result in the full case and the experimental value is quite good.

C. Calculated phase-shift parameters

Since our interest here is to study the coupling effects between the 1N + 3N and 2N + 2N (i.e., d+d, d+d*, d*+d*, d**+d, d**+d* and d**+d**) cluster configurations at energies around the d + d threshold, it is essential that the calculated threshold-energy difference Δ of the p+t and d+d channels be close to the experimental result. This is an important condition, because the strength of the coupling will certainly be sensitively dependent upon this particular difference. Unfortunately, however, the value of Δ obtained with the MN potential is only 1.67 MeV, which is appreciably smaller than the experimental value of 4.04 MeV. To correct this defect, we adjust the depth parameter V_{0s} of the singlet part in the MN potential [see Eq. (15) in Ref. 5] from 91.85 to 100.2 MeV. As a consequence of this adjustment, the triton parameters become

$$\lambda_1(t)=0.213\ \mathrm{fm}^{-2},\quad \lambda_2(t)=0.681\ \mathrm{fm}^{-2}, \tag{3.1}$$

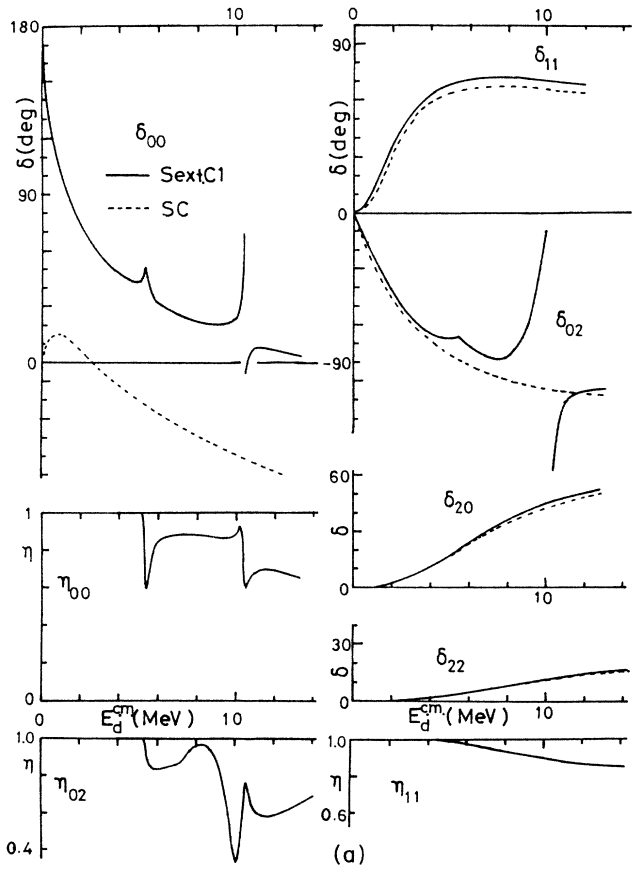

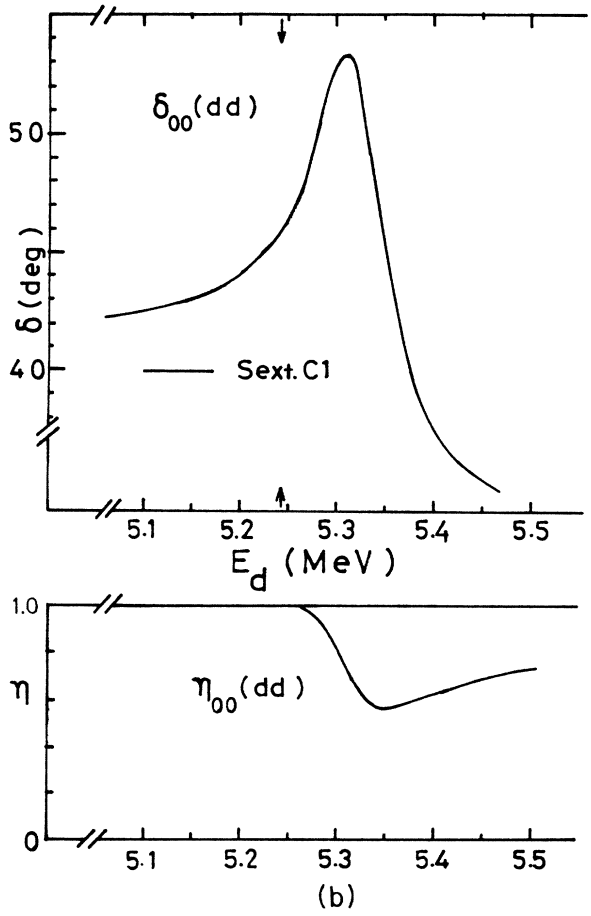

FIG. 2. (a) Comparison of calculated phase shifts δ_{ls} and reflection coefficients η_{ls} for d+d scattering in different cases. Solid and dotted curves represent calculated results in case Sext. C1 and SC, respectively. (b) An enlarged view of δ_{00} and η_{00} around the d* + d threshold.

and the ground-state energy is

$$\tilde{E}_3(t) = -8.20 \text{ MeV} , \quad (3.2)$$

thus yielding the desired value for Δ. We realize, of course, that this adjustment is somewhat arbitrary; however, considering that our aim is only to obtain a general understanding of the mutual influence of cluster configurations, we feel that this simple procedure is quite adequate.

The results depicted in Fig. 2(a), calculated with $V_{0s} = 100.2$ MeV, will now be discussed. First, we examine the specific distortion effect of the deuteron in d+d scattering. The calculations are carried out in two cases, SC and Sext. C1, and the spin-orbit part of the NN potential is omitted. The results for the phase shifts δ_{lS} in $l = 0$, 1, and 2 states are shown in this figure. Here one sees that in the $(lS) = (00)$ state distortion effects are large. The phase shift δ_{00} in case SC rises to a small positive value and then decreases monotonically, while that in case Sext.C1 shows a behavior indicating the presence of an additional bound state. Furthermore, the calculated phase shifts for the S state have rapidly varying or cusp-like structures which are produced by the coupling with pseudoinelastic channels (i.e., the d*+d configuration), and resonancelike structures arising from almost forbidden states[18] which will be smoothed out by the introduction of other channels or an imaginary potential into the calculation.[3]

In Fig. 2(b) we show an enlarged view of the $(lS) = (00)$ phase-shift and reflection-coefficient curves near the d*+d threshold, marked by an arrow on the abscissa. Here one notes the detailed structure of the rapidly varying behavior in the neighborhood of this threshold. Our opinion is that such a behavior occurs on account of the small Coulomb-barrier height in the d*+d channel caused by the large size of the d* cluster (see Table I).

In higher-l states, the situation is rather different. From Fig. 2(a) one finds that, already in the $(lS) = (11)$ state, the distortion effect is not large.

For the $S = 2$ state the 2N + 2N configuration is the

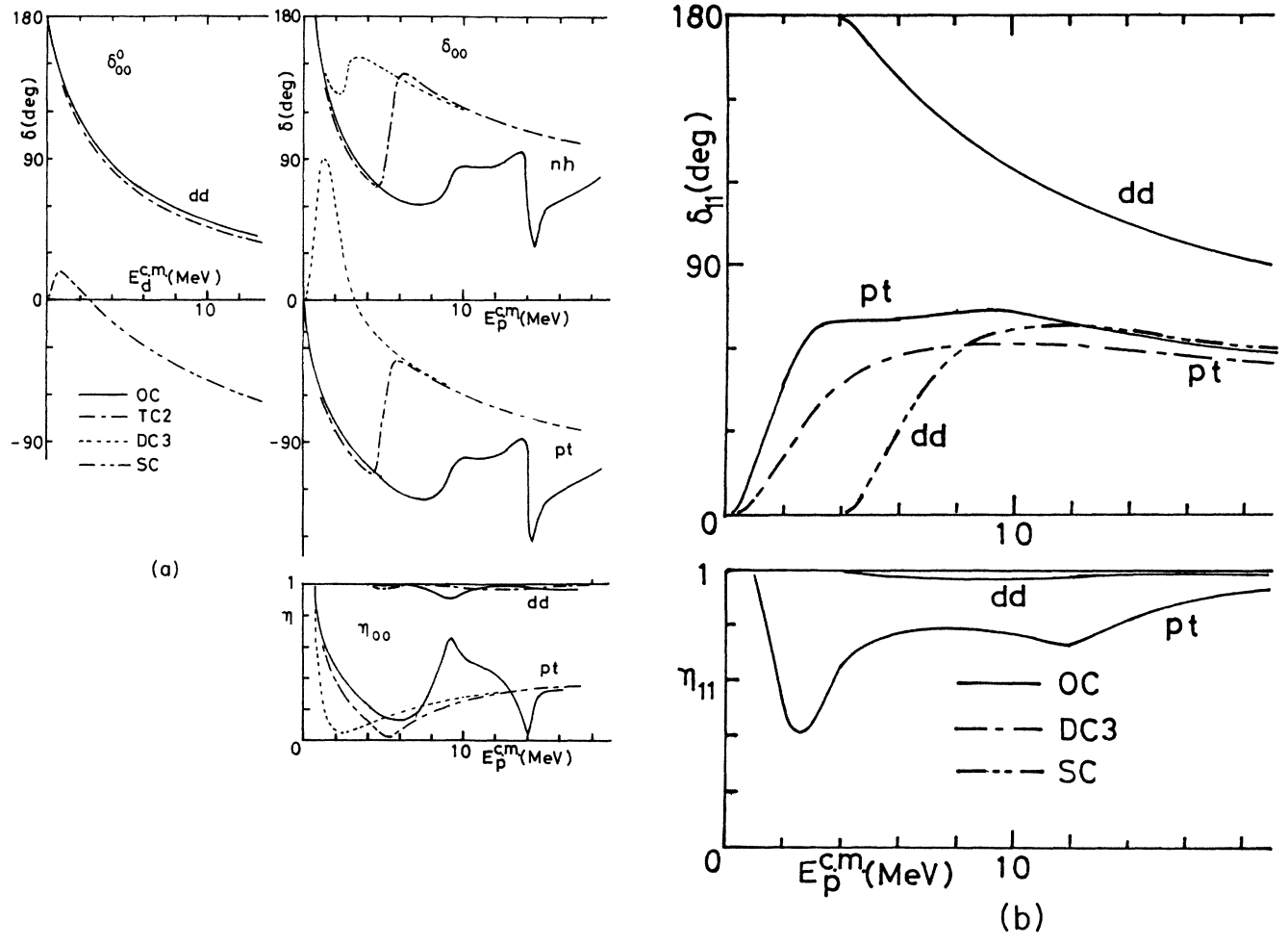

FIG. 3. (a) Comparison of calculated phase-shift parameters for d+d, p+t, and n+h elastic scattering in the $(lS) = (00)$ state. Solid, dotted-dashed, dotted, and double-dotted–dashed curves represent results calculated in cases OC, TC2, DC3, and SC, respectively. (b) Comparison of calculated phase-shift parameters for d+d and p+t elastic scattering in the $(lS) = (11)$ state. Solid, dotted-dashed, and double-dotted–dashed curves represent results calculated in cases OC, DC3, and SC, respectively.

energetically most favored cluster configuration and the 1N + 3N configuration does not contribute. Here, we carry out the calculation in 2N + 2N cases of single and sextuple configurations (SC and Sext.C1). The results obtained are also shown in Fig. 2(a). One sees from this figure that specific distortion effects for all states are rather small. In this respect, it is interesting to note that distortion effects in the $S=2$ state have never been considered previously.

Next, we examine the coupling effect of the 1N + 3N configuration, and the relation between channel-coupling and deuteron-distortion effects. The calculated phase-shift parameters (δ_{IS}^{J} and $\eta_{IS}^{J}=|S_{IS}^{J}|$) for d+d, p+t, and n+h elastic scattering and absolute values of S-matrix elements for the reactions ^{3}H(p,n)^{3}He in cases of DC3, TC2, and OC and ^{3}H(p,d)^{2}H in cases of TC2 and OC are shown in Figs. 3 and 4, respectively. From these figures, and Fig. 2, one can see the following characteristics in the calculated phase-shift parameters:

(i) The coupling between the 2N + 2N and 1N + 3N configurations is very strong, and so the calculated phase-shift parameters in all states for both d+d and p+t elastic scattering are strongly affected by introducing the coupling effect. In fact, in S-wave d+d scattering phase shifts, cusplike and resonancelike structures which are present in the 2N + 2N calculation disappear completely by taking into account the 1N + 3N configuration.

(ii) The rapidly changing behavior in the p+t scattering phase shift δ_{00} for the S wave near the n+h threshold disappears owing to the presence of a new bound state which is produced by introducing the coupling with the d+d configuration. Also, a resonancelike structure now appears around 5 MeV (see the TC2 curve).

(iii) In the p+t scattering phase shift for triplet P wave, the resonance is shifted to the lower-energy region and one more dispersionlike resonance structure appears by the coupling with the 2N + 2N configuration.

(iv) The influence of specific distortion, effected by including pseudoinelastic configurations involving pseudoexcited deuteron states, is clearly demonstrated in Fig. 3(a). Contrary to the case where the 2N + 2N configuration alone is considered [Fig. 2(a)], one notes that, with the inclusion of the 1N + 3N configuration, the effect of pseudoinelastic configurations on the d+d phase shift is rather weak. On the other hand, the S-wave phase shifts for p+t and n+h scattering are strongly affected by introducing pseudoinelastic configurations into the calculation. This is indicated by the large differences between the results in cases of TC2 and OC. The structures in δ and η parameters around 9 and 14 MeV are produced by coupling with the d*+d and d*+d* pseudoinelastic channels, respectively. This finding shows that the breakup effect of the deuteron is important in explaining the process of p+t or n+h scattering.

(v) Regarding the absolute values of the S-matrix elements for the ^{3}H(p,n)^{3}He reaction, the difference between the results in cases DC3 and OC is not too large in the singlet P state. On the other hand, for triplet P states, the differences are quite large, especially at low energies. This shows that the coupling effect of the d+d configuration in the p+t and n+h channels is very strong in triplet P

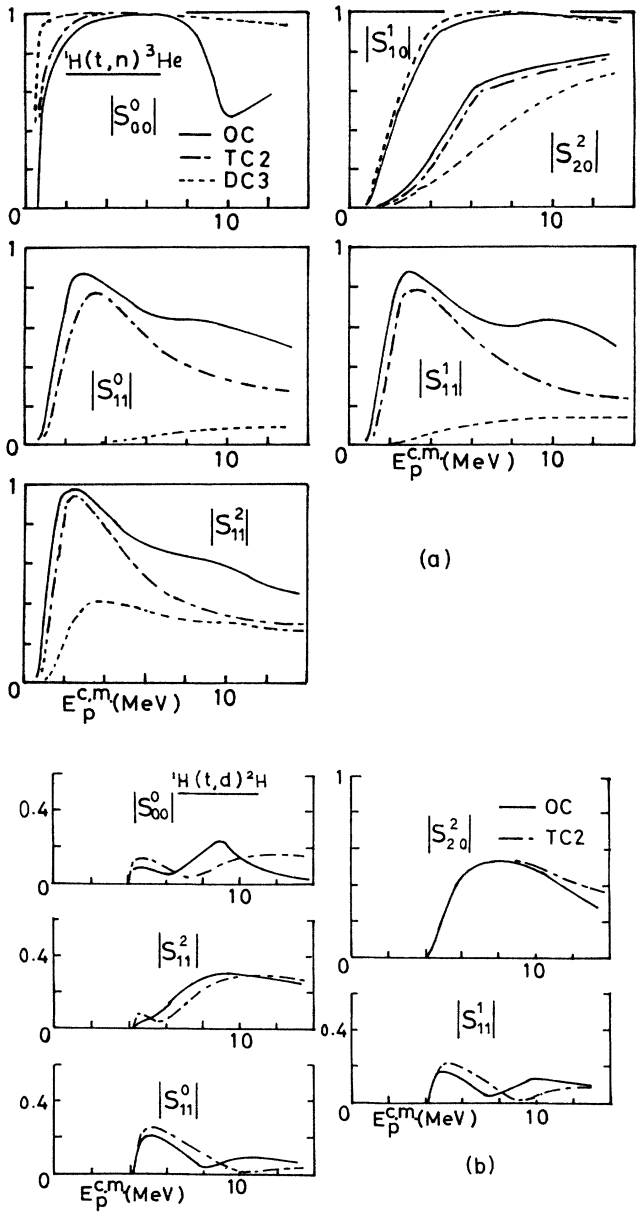

FIG. 4. (a) Comparison of calculated absolute values of S-matrix elements for the ^{3}H(p,n)^{3}He reaction. Solid, dotted-dashed, and dashed curves correspond to results obtained in cases OC, TC2, and DC3, respectively. (b) Same as (a), except that the reaction is ^{1}H(t,d)^{2}H.

states, which is caused essentially by the fact that in this calculation the resonance in the P state (negative-parity state) is very close to the threshold (4.03 MeV) of the d+d channel. The wavy structures in the full or OC case around 10 MeV are produced by introducing the coupling effect of the d*+d configuration.

(vi) As for the absolute values of the S-matrix elements for the ^{3}H(p,d)^{2}H reaction, we note from Fig. 4(b) that these values are not too large. Also, the difference between results in cases of TC2 and OC is small. These facts show that, at energies above the d+d threshold, the coupling between p+t and d+d configurations is not

very strong and the deuteron-distortion effect in this reaction is not large.

These findings indicate that, for a proper understanding of the characteristics of the ^{4}He scattering system, the most favored cluster configuration (1N + 3N) must always be taken into consideration.

D. Comparison with experimental data

In this subsection we compare calculated and experimental cross section and polarization results.

Differential cross sections can be calculated by using the phase-shift parameters obtained in each case of calculation. The results calculated for d+d elastic scattering at 2.23, 3.0, 4.2, 6.05, and 6.95 MeV in the c.m. system, p+t elastic scattering at 3.11, 5.33, 9.0, 10.2, 12.17, and 14.61 MeV in the c.m. system, and n + h elastic scattering at 4.5 MeV in the c.m. system, and two reactions ^{3}H(p,d)^{2}H at 10.2 MeV and ^{3}H(p,h)n at 7.1 and 10.2 MeV in the c.m. system are shown in Figs. 5(a) and 5(b), where a comparison with experimental data[19–21] is also made. From these figures one can see that for all processes the agreement between the results in the triple-configuration calculation (TC2: dotted-dashed curves) or the full calculation (OC: solid curves) and the experimental data (solid circles) is fairly satisfactory and becomes quite good especially at higher energies. In d+d scattering, the results in cases SC, Sext. C1, and OC are depicted in Fig. 5(a). Here one notes that the effect of specific distortion of the deuteron is rather small and that the coupling effect of the 1N + 3N configuration is important to reproduce the differential cross-section data. In p+t scattering, the results calculated in cases DC3, TC2, and OC are shown in Fig. 5(b). Here it is seen that the calculated results are quite satisfactory and become progressively better as the energy increases. Results obtained with a simpler calculation, utilizing only the 1N + 3N cluster configuration (dashed curves), are still reasonable; however, the improvement effected by the addition of the 2N + 2N configuration is easily noticeable.

The above discussion indicates that both 2N + 2N and 1N + 3N configurations play important roles in the ^{4}He scattering system.

The results calculated for ^{3}H(p,d)^{2}H reaction process at 10.2 MeV and for ^{3}H(p,n)^{3}He reaction process at 7.1 and 10.2 MeV are shown in Fig. 5(a). Here one notes that the OC calculation does reproduce rather well the essential features of the differential cross section data.

Polarizations for p+t and n+h elastic scattering are calculated by using the phase-shift parameters obtained. The calculated results are shown in Fig. 6, together with experimental data.[21,22] One can see from this figure that the agreement between the OC result and the experimental data is good except for the p+t case at 3.11 MeV. This is

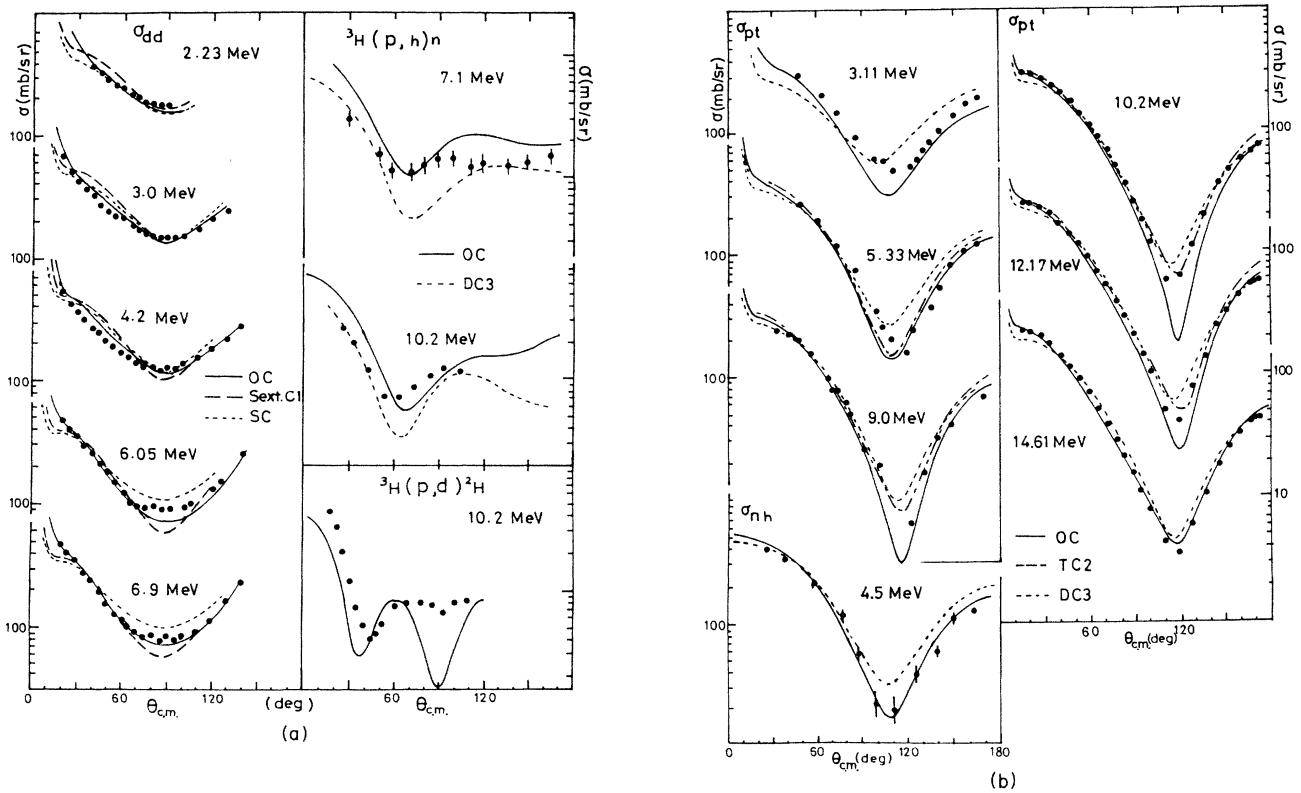

FIG. 5. (a) Comparison of calculated and experimental cross sections for d+d scattering, and ^{3}H(p,h)n and ^{3}H(p,d)^{2}H reactions. In the left-hand part, solid, dashed, and dotted curves represent results obtained in cases OC, Sext. C1, and SC, respectively. In the right-hand part, solid and dotted curves represent results obtained in cases OC and DC3, respectively. Solid circles represent experimental data. (b) Comparison of calculated and experimental cross sections for p+t and n+h scattering. Solid, dotted-dashed, and dotted curves represent results obtained in cases OC, TC2, and DC3, respectively.

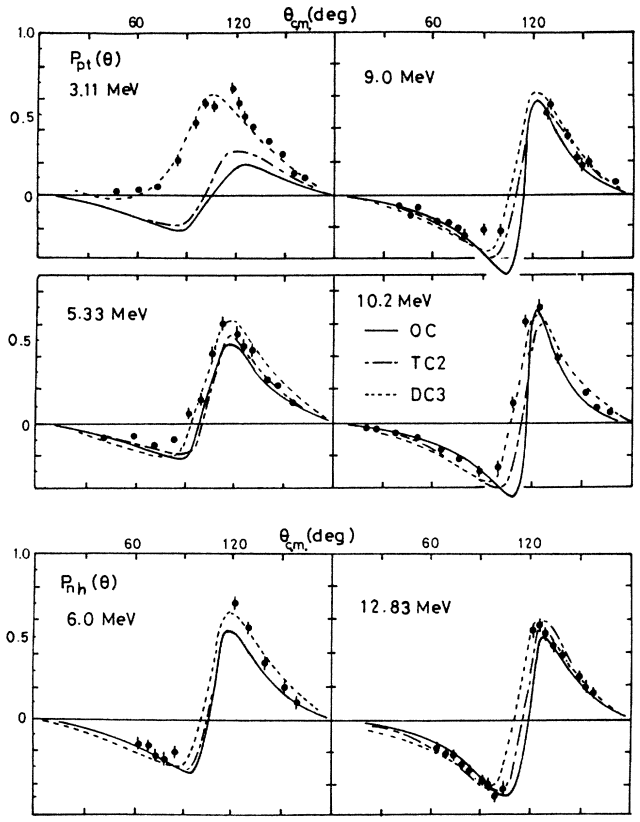

FIG. 6. Comparison of calculated and experimental polarizations for p+t and n+h scattering at various energies. Solid, dotted-dashed, and dotted curves have meanings similar to those indicated in Fig. 5(b).

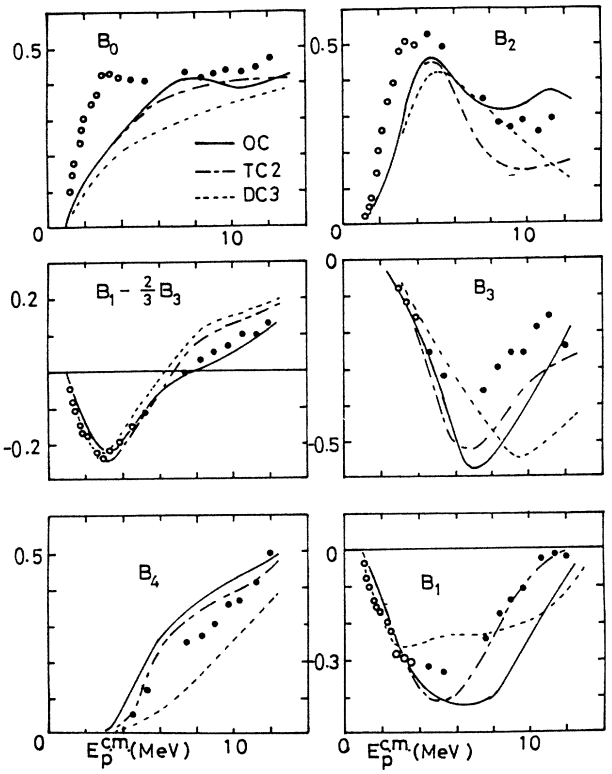

FIG. 7. Comparison of calculated and experimental expansion coefficients B_l of differential cross sections for ^{3}H(p,n)^{3}He reaction. Solid, dotted-dashed, and dashed curves represent results obtained in cases OC, TC2, and DC3, respectively. Solid and open circles represent experimental values obtained by Smith *et al.* and McDaniels *et al.*, respectively (Ref. 24).

rather satisfying, since our NN potential contains no adjustable parameters not only in the central part but also in the spin-orbit part. Together with the differential cross-section comparison discussed above, we may conclude that, at energies where the splitting of the ^3P phases due to noncentral forces is important, the crude representation of tensor effects by an effective NN spin-orbit force is not sufficient[7] and, as a consequence, the calculated results become less satisfactory in the lower-energy region.

Now, to see the effect of deuteron distortion in the ^{3}H(p,n)^{3}He reaction process at low energies, we examine the Legendre coefficients B_l which can be calculated by using the values of the calculated S-matrix elements (see Refs. 7 and 23). Calculated values in the cases DC3, TC2, and OC, and empirical values[24] are shown in Fig. 7. One can see from this figure that in cases TC2 and OC the agreement of the calculated results with experiment is better as a whole than in case DC3. The discrepancy between the results in case TC2 or OC and experiment for B_0 and B_2 at low energies comes from the fact that the splitting in the triplet P states is not too realistic owing to the representation of tensor effects by an effective NN spin-orbit potential.

It should be mentioned that the NN potential adopted in this calculation is very similar to that required in p+α, d+α, ^{3}H + α, and α+α systems. Also, no phenomenological imaginary potentials are included in the formulation.

IV. CONCLUDING REMARKS

In this investigation the main purpose is to examine the effects of specific distortion and channel coupling in the ^{4}He system. The results show that, for a proper understanding of the characteristics of this system, the energetically most favored cluster configuration, that is, the 1N + 3N configuration, must always be taken into consideration, and that the 2N + 2N configuration with specific distortion effects must also be taken into account. A proper consideration of both 1N + 3N and 2N + 2N configurations is found to be necessary for a satisfactory description of experimental data on the level structure of positive-parity states including the ground state and the differential cross sections and polarizations for d+d, p+t, and n+h scattering and the differential cross sections for ^{3}H(p,d)^{2}H and ^{3}H(p,h)n reactions.

Another finding from this investigation is that in the case where the energetically most favored 1N + 3N configuration is included, the specific distortion effect of the deuteron cluster is rather reduced. This shows that in a calculation which neglects the energetically most favored configuration, the specific distortion effect is increased to

compensate partially for the defect in the calculation. Together with results obtained from similar studies in other light systems, one can now conclude that specific distortion effects will be important only when readily compressible clusters are involved in the system and can be reliably studied only when there are no energetically more favored configurations which, in actuality, must be taken into consideration in the calculation.

Furthermore, one finds from this study that it is appropriate to adopt an effective NN potential which is very similar to that required in the $p+\alpha$, $d+\alpha$, $^3H+\alpha$, and $\alpha+\alpha$ systems. This is very interesting from the viewpoint of achieving a unified description of the main features of all light systems by adopting a single effective NN potential.

There are some improvements which should be made. One of these is to adopt a more realistic NN potential in which the tensor part is included. Furutani[7] has shown from his microscopic two-channel calculation that the tensor term of the NN potential plays a significant role to reproduce the $1N+3N$, $T=1$ scattering properties [p+t and n+h scattering, and $^3H(p,n)^3He$ reaction]. Another improvement is to take account of the full breakup effect of the deuteron cluster. In our calculation, the virtual breakup effect[3] is considered by introducing excited pseudostates of the deuteron and channel coupling with the $1N+3N$ configuration. However, this may not be quite sufficient, because only two pseudoexcited states of the deuteron cluster are introduced in the present study.[3] For a more satisfactory description, one may need to consider many deuteron pseudostates, including also those in singlet configurations.

[1]H. Kanada, T. Kaneko, and Y. C. Tang, Nucl. Phys. **A389**, 285 (1982).
[2]H. Kanada, T. Kaneko, M. Nomoto, and Y. C. Tang, Prog. Theor. Phys. **72**, 369 (1984).
[3]H. Kanada, T. Kaneko, S. Saito, and Y. C. Tang, Nucl. Phys. **A444**, 209 (1985).
[4]D. R. Thompson, M. LeMere, and Y. C. Tang, Nucl. Phys. **A286**, 53 (1977).
[5]H. Kanada, T. Kaneko, and Y. C. Tang, Nucl. Phys. **A380**, 87 (1982).
[6]P. Heiss, B. Bauer, H. Aulenkamp, and H. Stöwe, Nucl. Phys. **A286**, 42 (1977); H. M. Hofmann, W. Zahn, and H. Stöwe, *ibid.* **A357**, 139 (1981).
[7]H. Furutani, Prog. Theor. Phys. **65**, 586 (1981).
[8]D. R. Thompson, Nucl. Phys. **A143**, 304 (1970).
[9]Y. Mito and M. Kamimura, Prog. Theor. Phys. **56**, 583 (1976); M. Kamimura, Prog. Theor. Phys. Suppl. **62**, 236 (1977).
[10]R. D. Furber, Ph.D. thesis, University of Minnesota, 1976.
[11]T. A. Tombrello, Phys. Rev. **138**, 1340 (1965).
[12]A preliminary account of this work was given by H. Kanada and Y. C. Tang, in Proceedings of the International Symposium on Few-Body Methods, Nanning, Quangxi, People's Republic of China (1985). Because of a small computational error, the results reported there were slightly inaccurate. The inaccuracy was, however, quite minor and does not affect the conclusions made.
[13]M. Sakai, Prog. Theor. Phys. **63**, 180 (1980).
[14]P. Szydlik and C. Werntz, Phys. Rev. **138**, B866 (1965).
[15]S. Fiarman and W. E. Meyerhof, Nucl. Phys. **A206**, 1 (1973).
[16]R. Hofstadter, Ann. Rev. Nucl. Sci. **7**, 231 (1957).
[17]H. Frank, O. Haas, and H. Prange, Phys. Lett. **19**, 391 (1985); **19**, 719 (1965).
[18]S. Saito, S. Okai, R. Tamagaki, and M. Yasuno, Prog. Theor. Phys. **50**, 1561 (1973).
[19]R. Kankowsky, J. C. Fritz, K. Kilian, A. Neufert, and D. Fick, Nucl. Phys. **A263**, 29 (1976).
[20]J. E. Brolley, Jr., T. M. Putnam, L. Rosen, and L. Stewart, Phys. Rev. **117**, 1307 (1960).
[21]J. L. Detch, R. L. Hutson, N. Jarmie, and J. H. Jett, Phys. Rev. C **4**, 52 (1971).
[22]W. E. Wilson, R. L. Walter, and D. B. Fossan, Nucl. Phys. **27**, 421 (1961).
[23]C. Werntz and W. E. Meyerhof, Nucl. Phys. **A121**, 38 (1968).
[24]J. R. Smith and S. T. Thornton, Nucl. Phys. **A186**, 161 (1972); D. K. McDaniels, M. Drosg, J. C. Hopkins, and J. D. Seagrave, Phys. Rev. C **6**, 1593 (1972).